The crust of isolated and accreting neutron stars

Leszek Zdunik

collaboration with Paweł Haensel, Morgane Fortin (CAMK), Nicolas Chamel, Anthea Fantina (ULB, Brussels)

CAMK - Nicolaus Copernicus Astronomical Center
Warsaw, Poland

jlz@camk.edu.pl

XXXIX International Conference of Theoretical Physics
Matter to the Deepest
Ustroń, 17 September 2015

Neutron Star

Structure

- outer crust
  Nuclei + electron gas
- inner crust
  Nuclei + neutron gas + electron gas
- core
  neutron + protons + electrons + miuons
- inner core
  + hyperons + quarks + ??

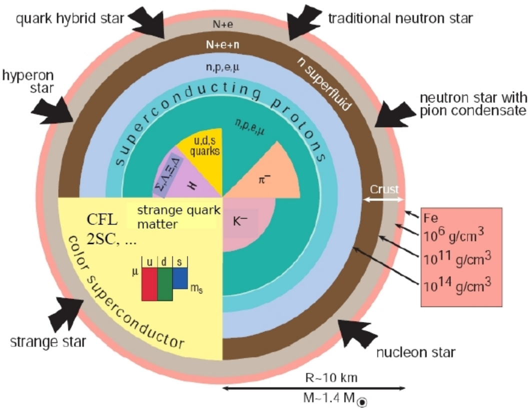

Figure - Fridolin Weber

Units

- 1 MeV/fm^3 = $1.6022 \cdot 10^{33}$ erg/cm^3
- 1 MeV/fm^3 = $1.7827 \cdot 10^{12}$ g/cm^3
- $n_s = 0.16$ fm^{-3}

Location in NS	n_b		Mass-energy ρ		Pressure P		Chem. pot. μ_b
Center max	$7.4 n_0$	1.2	1575	$2.81\,10^{15}$	830	$1.33\,10^{36}$	2000
Center typical	$3.4 n_0$	0.54	550	$9.78\,10^{14}$	84	$1.34\,10^{35}$	1200
Crust/core	$0.5 n_0$	0.077	80	$1.4\,10^{14}$	0.33	$5.36\,10^{32}$	944
Inner/outer crust	$0.001 n_0$	$2.5\,10^{-4}$	0.25	$4.3\,10^{11}$	$6\,10^{-4}$	10^{30}	940

Two *kinds* of the NS crust - formation scenario

- NS born in SN explosion - collapse of stellar core
  NS born at high temperature $\sim 10^{11}$ K
  star (including crust) in thermodynamical equilibrium - all reactions possible
  catalyzed crust - ground state of matter
  no exothermic reactions possible
- accreting NS - accretion of matter on neutron star
  temperature not so high $\leq 10^{9}$ K
  no energy to overcome Coulomb barrier for nuclei (relatively large $Z > 10$)
  system is in local (not global) minimum of energy
  accreted crust - source of non-equilibrium (exothermic) reactions
  energy reservoir

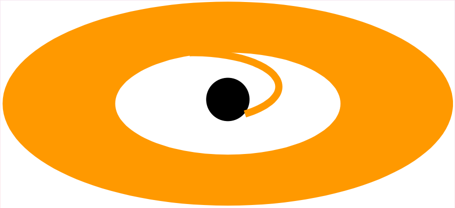

Structure of the catalyzed crust

State of matter defined by the global minimum of the energy of a system.
Equivalently - energy density - per particle (per baryon)

Outer crust $\rho < 4\,10^{11}$ g cm^{-3}

- onion-like structure
- nuclei in the electron gas
- Z decreases inwards $Z_1 > Z_2 > Z_3$ - neutronization
- neutron drip at the bottom of the outer crust

Inner crust $\rho > 4\,10^{11}$ g cm^{-3}

- onion-like structure
- nuclei in the electron and neutron gas
- Z decreases inwards $Z_1 > Z_2 > Z_3 > Z_4 \ldots$ - neutronization

P increases $\Longrightarrow A$ increases
P increases $\Longrightarrow Z/A$ decreases

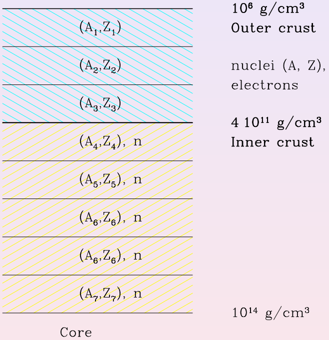

Structure of the accreted crust

- some reactions not allowed due to physical conditions (low temperature - thermonuclear reactions blocked)
- additional constraints in thermodynamic equilibrium
- impossible to reach global minimum of energy (Gibbs energy at given pressure) - local minimum of energy
- system in local equilibrium - energy reservoir - exothermic reactions possible
- energy sources in the inner crust - few hundreds meters below NS surface
- timescale of heat transfer to the surface - years,
- additional luminosity source when accretion stops
- total crustal heating is $\sim 1.5 - 2$ MeV per one accreted nucleon, mostly deposited at $\rho \sim 10^{12} - 10^{13}$ g cm^{-3}

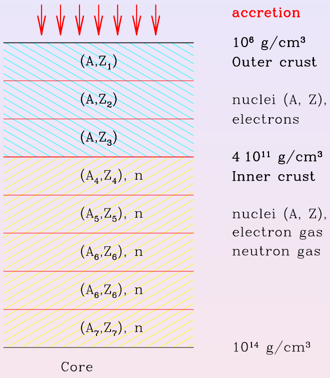

Thermodynamics

Assumptions

- One-component plasma: a single nuclear species (N, Z) is present at each pressure.
- Properties of the matter calculated for the Wigner-Seitz cells containing one nucleus and A nucleons (above neutron drip point - neutron gas outside nuclei)

Determination of the state of matter

At given pressure P:

- Gibbs energy per one cell - $G_{\mathrm{cell}}(A, Z)$.
- Gibbs energy per nucleon $g = G_{\mathrm{cell}}/A = \mu_{\mathrm{b}}(A, Z)$ the baryon chemical potential for a given nuclide.
- ground state $\equiv$ minimum of $\mu_{\mathrm{b}}(A, Z)$ at fixed P with bounds corresponding to specific physical situation.
  – accreted crust – with respect to neighboring $N, Z; \quad A = \mathrm{const.}$
  – catalyzed crust – minimal μ_{b} with respect to A and Z.

Most important ingredient - the binding energies of a nuclei.

Nuclei in Neutron Star crust vs measured masses

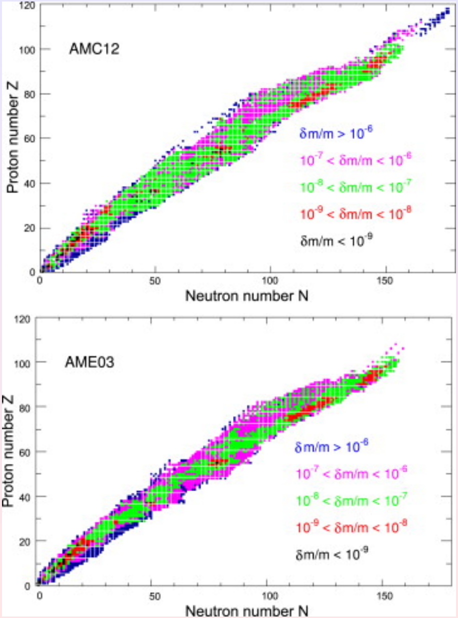

- Only few crust nuclei "measured" in experiment.
- Theoretical models fitted to experiment

Nuclear charts with relative mass uncertainties $\delta m/m$ displayed in a color code for AMC12 (top) and for AME03(bottom)

B. Pfeiffer, K. Venkataramaniah, U. Czok, C. Scheidenberger

Atomic mass compilation 2012

Atomic Data and Nuclear Data Tables, Volume 100, Issue 2, March 2014, Pages 403-535

Nuclei in Neutron Star crust vs measured masses

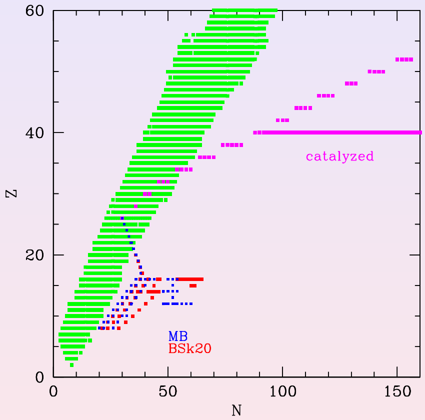

- Only few crust nuclei “measured” in experiment.
- Theoretical models fitted to experiment

Nuclear charts with relative mass uncertainties $\delta m/m$ displayed in a color code for AMC12 (top) and for AME03(bottom)

B. Pfeiffer, K. Venkataramaniah, U. Czok, C. Scheidenberger

Atomic mass compilation 2012

Atomic Data and Nuclear Data Tables, Volume 100, Issue 2, March 2014, Pages 403-535

Nuclei in Neutron Star crust vs measured masses

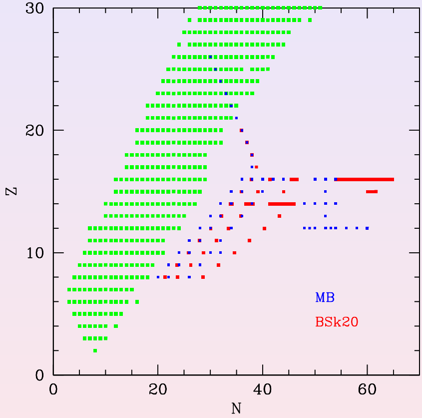

- Only few crust nuclei "measured" in experiment.
- Theoretical models fitted to experiment

Nuclear charts with relative mass uncertainties $\delta m/m$ displayed in a color code for AMC12 (top) and for AME03(bottom)

B. Pfeiffer, K. Venkataramaniah, U. Czok, C. Scheidenberger

Atomic mass compilation 2012

Atomic Data and Nuclear Data Tables, Volume 100, Issue 2, March 2014, Pages 403-535

Mackie & Baym model - Compressible Liquid Drop Model 1977

Nucleus (drop) and gas (neutron) outside treated separately
$P > P_{ND} \equiv P(\rho_{ND})$, neutrons in two phases:
– bound in nuclei
– as a neutron gas outside nuclei.
The Gibbs energy of the W-S cell:

$$G_{\rm cell}(A,Z) = W_{\mathcal{N}}(A,Z,n_n) + W_L(n_{\mathcal{N}},Z) + [\mathcal{E}_e(n_e) + (1-n_{\mathcal{N}}V_{\mathcal{N}})\,\mathcal{E}_n(n_n) + P]/n_{\mathcal{N}}\ ,$$

$W_{\mathcal{N}}$ – the energy of the nucleus, $W_{\mathcal{N}} = W_{bulk} + W_{surf} + W_{Coul} + W_{pair}$
W_L – the lattice energy per cell
$\mathcal{E}_e$ – the electron energy density.
$\mathcal{E}_n$ – energy density of neutron gas outside nuclei, $V_{\mathcal{N}}$ – volume of the nucleus.
At given nuclide (A,Z) — system described by $n_{\mathcal{N}},\ n_e,\ n_n$

Even-odd pairing energy - important ingredient of $W_{\mathcal{N}}(A,Z)$:

$$W_{pair} = \frac{1}{2}\left[(-1)^N + (-1)^Z\right]\frac{11}{\sqrt{A}}\ \mathrm{MeV}$$

Even-even nuclei (N,Z) are thermodynamically preferred.

BSk (Brussels-Skyrme) model 2012

- Extended Thomas Fermi method
- Skyrme type forces
- no separation of matter into 2 distinct homogeneous phases
- Z well defined for proton cluster
- neutron skin - N_{cell} well determined, not N - neutron number bound by the proton cluster
- continuous variation of the density of nuclear matter within WS cell
- self-consistent treatment of surface layer
- shell effects for protons included - Z magic numbers preferred
- no even-odd pairing

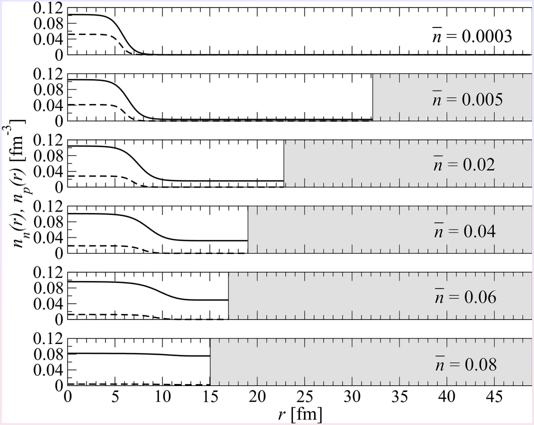

Profiles of neutron (solid curves) and proton (dashed curves) density distributions in the Wigner-Seitz cell for functional BSk21 and different values of the mean density $\bar{n}$. Shading denotes the region beyond the cell radius

Pearson, Chamel, Goriely, Ducoin 2012

Accreting crust - evolution od matter element

$P_1 < P_2 < P_3$, $\mu - \mu_{\rm cat}$ energy per baryon relative to ground state (catalyzed matter)

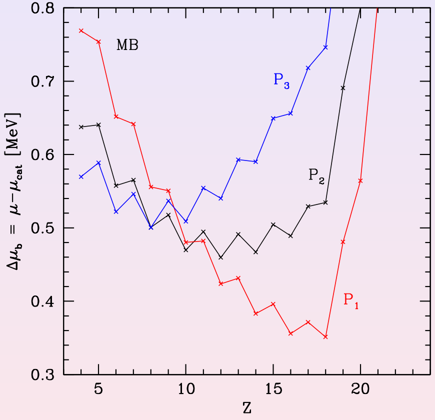

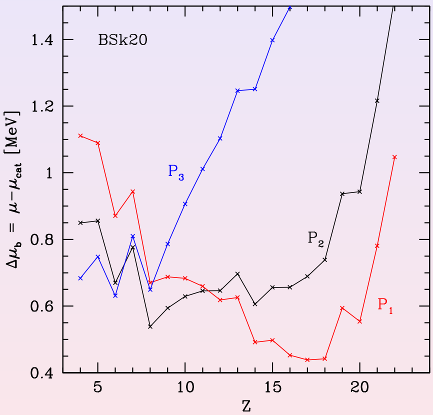

pairing energy,
even Z energetically preferred
increasing $P \to Z$ decreases by 2

shell effects, deeper minima,
magic numbers Z energetically preferred
Z slips from 20 to 14, then to 8

Outer crust - Nuclei (N,Z)

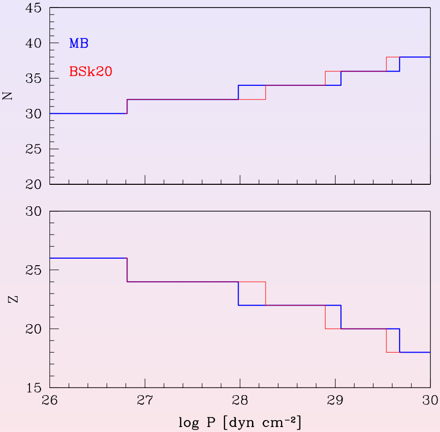

Three first stable nuclei experimentally "measured"
(5 nuclei including beta-unstable)

Increasing pressure of the Wigner-Seitz cell P
threshold to be reached:

$$\mu_e + \mu_{\mathcal{N}(A,Z)} = \mu_{\mathcal{N}(A,Z-1)}$$

The electron captures proceed in two steps,

$$(A,Z) + e^- \longrightarrow (A,Z-1) + \nu_e \ ,$$

$$(A,Z-1) + e^- \longrightarrow (A,Z-2) + \nu_e + Q_c \ .$$

$\Downarrow$

decrease of Z (increase of $N = A - Z$) with increasing density.
The first capture – in quasi-equilibrium $\rightarrow$ negligible energy release.

$\Downarrow$

odd-odd nucleus (strongly unstable)

$\Downarrow$

a second electron capture in an non-equilibrium manner, with energy release Q_c.

Deep heat sources - model comparison - outer crust

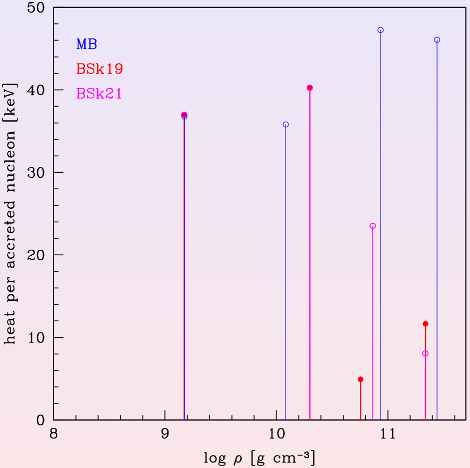

Vertical lines, positioned at the density at the bottom of the reaction shell, represent the heat per one accreted nucleon

Two first (low density) energy sources correspond to the nuclei experimentally "measured"
model dependence at higher densities

Inner crust reactions

Above the neutron-drip point ($\rho > \rho_{\rm ND}$) electron captures trigger neutron emissions

MB - compressible liquid drop model

The condition for the beta capture:

$$\mu_b(P, A_{\rm cell}, N, Z) = \mu_b(P, A_{\rm cell}, N', Z-1)$$

where the number of neutrons in nucleus N' corresponds to the minimum of μ_b with respect to N i.e. $\forall_{N \neq N'} \;\; \mu_b(P, A_{\rm cell}, N', Z-1) < \mu_b(P, A_{\rm cell}, N, Z-1)$.
For each Z - equilibrium with respect to strong interactions allowing for neutron drip out of nuclei and changing neutron gas density (outside nuclei).

BSk

Finding the points (in pressure) at which the condition is fulfilled:

$$\mu_b(P, A_{\rm cell}, Z) = \mu_b(P, A_{\rm cell}, Z-1)$$

This reaction ($Z \to Z-1$) trigger exothermic electron capture: ($Z-1 \to Z-2$) and sometimes the chain of subsequent pairs of beta reactions leading finally to Z-even nucleus.

quasi equilibrium

$$(A_{\rm cell}, Z) + e^- \longrightarrow (A_{\rm cell}, Z-1) + \nu_e (+k'n)$$

a second electron capture and neutron emissions in a non-equilibrium manner, with energy release Q.

$$(A_{\rm cell}, Z-1) + e^- \longrightarrow (A_{\rm cell}, Z-2) + {\rm k}\; n + \nu_e + Q$$

Inner crust - nuclei (N,Z)

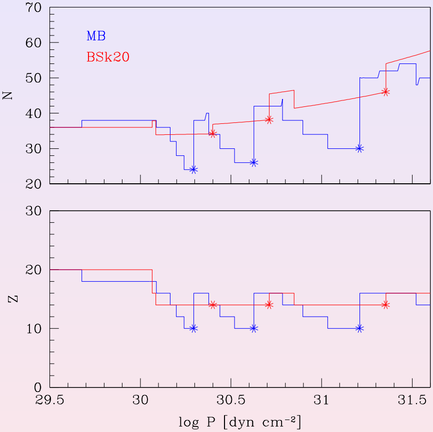

stars - pycnonuclear fusion
- Z decreases with increasing density.

$\Downarrow$

Coulomb barrier prohibiting the nucleus-nucleus reaction lowers.
Decrease of the separation between the neighboring nuclei,
Increase of energy of the quantum zero-point vibrations around the nuclear lattice sites

$\Downarrow$

Pycnonuclear reactions.

$$(A,Z) + (A,Z) \longrightarrow (2A,2Z) + Q_1 \ ,$$
$$(2A,2Z) \longrightarrow (2A-\mathrm{k},2Z) + \mathrm{k}\ n + Q_2 \ ,$$

MB - odd-even pairing energy
even Z energetically preferred
BSk - shell effects
$Z = Z_{shell}$ energetically preferred

Deep heat sources - model comparison - inner crust

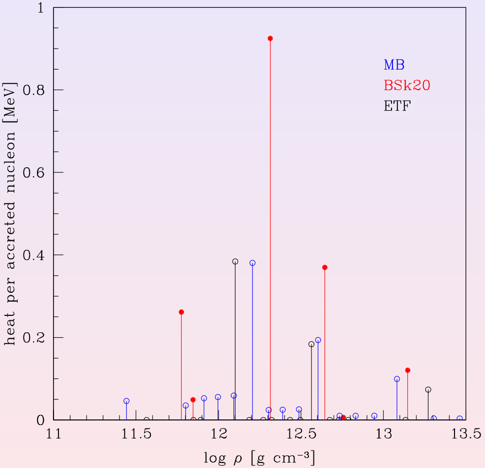

Vertical lines, positioned at the density at the bottom of the reaction shell, represent the heat per one accreted nucleon

MB - pairing - many heat sources, small energy per one source

BSk - shell effects - small number of sources ($\approx N_{pair}/3$), large energy per one source

ETF - no paring, no shell correction - leads to equilibrium-electron captures (no heat release), heating results exclusively from pycno-nuclear fusion

Reactions

Non-equilibrium processes in the **outer crust** of an accreting neutron stars assuming that the X-ray ashes consist of pure ^{56}Fe.

P (dyn cm^{-2})	ρ (g cm^{-3})	Reactions	X_n	$\Delta\rho/\rho$	μ_e	q (keV)
7.23×10^{26}	1.49×10^{9}	$^{56}\mathrm{Fe} \rightarrow^{56}\mathrm{Cr} - 2e^- + 2\nu_e$	0	0.08	4.08	40.7
9.57×10^{27}	1.11×10^{10}	$^{56}\mathrm{Cr} \rightarrow^{56}\mathrm{Ti} - 2e^- + 2\nu_e$	0	0.09	8.18	35.8
1.15×10^{29}	7.85×10^{10}	$^{56}\mathrm{Ti} \rightarrow^{56}\mathrm{Ca} - 2e^- + 2\nu_e$	0	0.10	15.64	47.3
4.75×10^{29}	2.50×10^{11}	$^{56}\mathrm{Ca} \rightarrow^{56}\mathrm{Ar} - 2e^- + 2\nu_e$	0	0.11	22.48	46.1
1.36×10^{30}	6.11×10^{11}	$^{56}\mathrm{Ar} \rightarrow^{52}\mathrm{S} + 4n - 2e^- + 2\nu_e$	0	0.12	29.38	59.8
1.980×10^{30}	9.075×10^{11}	$^{52}\mathrm{S} \rightarrow^{46}\mathrm{Si} + 6n - 2e^- + 2\nu_e$	0.07	0.13	32.27	128.0

Reactions

Non-equilibrium processes in the inner crust.

P (dyn cm^{-2})	ρ (g cm^{-3})	Reactions	X_n	$\Delta\rho/\rho$	μ_e	q (keV)
2.253×10^{30}	1.131×10^{12}	$^{46}\mathrm{Si} \rightarrow ^{40}\mathrm{Mg} + 6n - 2e^- + 2\nu_e$	0.18	0.14	32.22	143.5
2.637×10^{30}	1.455×10^{12}	$^{40}\mathrm{Mg} \rightarrow ^{34}\mathrm{Ne} + 6n - 2e^- + 2\nu_e$				
		$^{34}\mathrm{Ne} + ^{34}\mathrm{Ne} \rightarrow ^{68}\mathrm{Ca}$	0.39	0.17	34.34	507.9
2.771×10^{30}	1.766×10^{12}	$^{68}\mathrm{Ca} \rightarrow ^{62}\mathrm{Ar} + 6n - 2e^- + 2\nu_e$	0.45	0.8	34.47	65.8
3.216×10^{30}	2.134×10^{12}	$^{62}\mathrm{Ar} \rightarrow ^{56}\mathrm{S} + 6n - 2e^- + 2\nu_e$	0.45	0.09	35.47	71.6
3.825×10^{30}	2.634×10^{12}	$^{56}\mathrm{S} \rightarrow ^{50}\mathrm{Si} + 6n - 2e^- + 2\nu_e$	0.50	0.09	36.59	77.9
4.699×10^{30}	3.338×10^{12}	$^{50}\mathrm{Si} \rightarrow ^{44}\mathrm{Mg} + 6n - 2e^- + 2\nu_e$	0.55	0.09	37.89	84.6
6.043×10^{30}	4.379×10^{12}	$^{44}\mathrm{Mg} \rightarrow ^{36}\mathrm{Ne} + 8n - 2e^- + 2\nu_e$				
		$^{36}\mathrm{Ne} + ^{36}\mathrm{Ne} \rightarrow ^{72}\mathrm{Ca}$				
		$^{72}\mathrm{Ca} \rightarrow ^{66}\mathrm{Ar} + 6n - 2e^- + 2\nu_e$	0.61	0.14	39.41	308.8
7.233×10^{30}	5.839×10^{12}	$^{66}\mathrm{Ar} \rightarrow ^{60}\mathrm{S} + 6n - 2e^- + 2\nu_e$	0.70	0.04	39.01	29.5
9.238×10^{30}	7.041×10^{12}	$^{60}\mathrm{S} \rightarrow ^{54}\mathrm{Si} + 6n - 2e^- + 2\nu_e$	0.73	0.04	40.34	31.0
1.228×10^{31}	8.980×10^{12}	$^{54}\mathrm{Si} \rightarrow ^{48}\mathrm{Mg} + 6n - 2e^- + 2\nu_e$				
		$^{48}\mathrm{Mg} + ^{48}\mathrm{Mg} \rightarrow ^{96}\mathrm{Cr}$				
		$^{96}\mathrm{Cr} \rightarrow ^{94}\mathrm{Cr} + 2n$	0.80	0.04	41.86	135.1
1.463×10^{31}	1.057×10^{13}	$^{94}\mathrm{Cr} \rightarrow ^{88}\mathrm{Ti} + 6n - 2e^- + 2\nu_e$	0.81	0.02	41.99	11.5
1.816×10^{31}	1.254×10^{13}	$^{88}\mathrm{Ti} \rightarrow ^{82}\mathrm{Ca} + 6n - 2e^- + 2\nu_e$	0.82	0.02	43.18	11.3
2.304×10^{31}	1.506×10^{13}	$^{82}\mathrm{Ca} \rightarrow ^{76}\mathrm{Ar} + 6n - 2e^- + 2\nu_e$	0.84	0.02	44.48	10.9
2.998×10^{31}	1.838×10^{13}	$^{76}\mathrm{Ar} \rightarrow ^{70}\mathrm{S} + 6n - 2e^- + 2\nu_e$	0.85	0.02	45.91	10.0
4.028×10^{31}	2.287×10^{13}	$^{70}\mathrm{S} \rightarrow ^{64}\mathrm{Si} + 6n - 2e^- + 2\nu_e$				
		$^{64}\mathrm{Si} + ^{64}\mathrm{Si} \rightarrow ^{128}\mathrm{Ni}$				
		$^{128}\mathrm{Ni} \rightarrow ^{126}\mathrm{Ni} + 2n$	0.87	0.01	47.48	67.3
5.278×10^{31}	2.784×10^{13}	$^{126}\mathrm{Ni} \rightarrow ^{124}\mathrm{Fe} + 2n - 2e^- + 2\nu_e$	0.88	0.01	48.50	2.5
7.311×10^{31}	3.493×10^{13}	$^{124}\mathrm{Fe} \rightarrow ^{122}\mathrm{Cr} + 2n - 2e^- + 2\nu_e$	0.89	0.01	51.05	2.4

Integrated heat

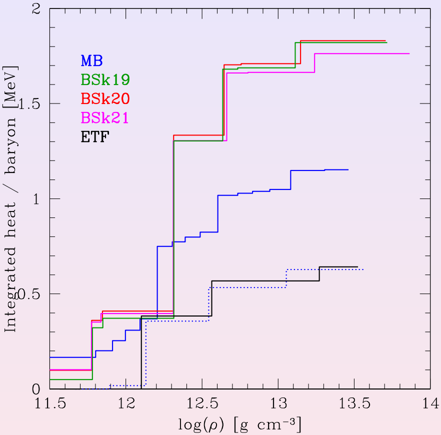

Integrated heat - heat deposited in the crust in the layer with density $< \rho$

$$Q(\rho) = \sum_{j(\rho_j < \rho)} Q_j,$$

$Q(\rho)$ (per one accreted nucleon) versus ρ, assuming initial ashes of pure ^{56}Fe.

ETF - pure Extended Thomas-Fermi no Pairing, no Shell Corrections

Weak dependence of $Q_{\rm tot}$ on the "nuclear history", dense matter model
Crucial role of pairing and shell effects for $Q_{\rm tot}$ - for ETF $Q_{\rm tot}$ is three times smaller

$$Q_{MB} \simeq 2 \cdot Q_{ETF} \qquad Q_{BSk} \simeq 3 \cdot Q_{ETF}$$

EOS - accreted crust vs. ground-state (catalyzed)

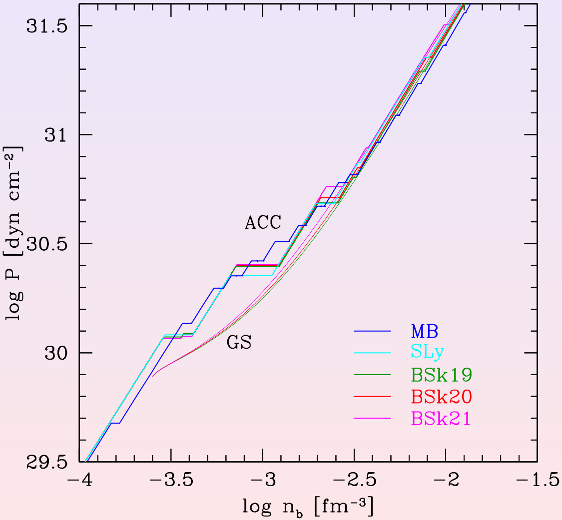

For:
$n_{\rm b} \in (3 \cdot 10^{-4} \div 3 \cdot 10^{-3})\ {\rm fm}^{-3}$
$\rho \in (5 \cdot 10^{11} \div 5 \cdot 10^{12})\ {\rm g\ cm}^{-3}$
accreted crust is significantly stiffer than the ground state (catalyzed)

Neutron Star parameters

- crust structure does not influence maximum mass of Neutron Star
- Typically: $M = 1.4\ \mathrm{M}_\odot$, $R_{\mathrm{ACC}} - R_{\mathrm{GS}} \approx 100$ m.
- This difference decreases with increasing M.
- $M = 1.0 M_\odot$ - 200 m
  $M = 1.4 M_\odot$ - 100 m
  $M = 1.7 M_\odot$ - 50 m
- the relative effect for the thickness of a crust 10%
  Total crust thickness $\Delta R_{\mathrm{crust}}$:
  $M = 1.0 M_\odot$ - 2 km
  $M = 1.4 M_\odot$ - 1 km
  $M = 1.7 M_\odot$ - 500 m

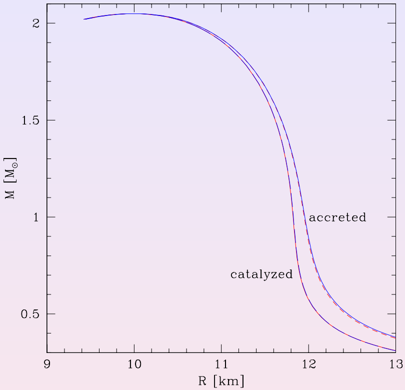

- the difference in radius due to the formation scenario (accreted vs catalyzed crust) much smaller than the effect of the EOS in the core.
- observational inaccuracy of a measurement of a radius of NS larger than 2 km

Neutron Star parameters

- crust structure does not influence maximum mass of Neutron Star
- Typically: $M = 1.4\ \mathrm{M}_\odot$, $R_{\mathrm{ACC}} - R_{\mathrm{GS}} \approx 100$ m.
- This difference decreases with increasing M.
- $M = 1.0M_\odot$ - 200 m
  $M = 1.4M_\odot$ - 100 m
  $M = 1.7M_\odot$ - 50 m
- the relative effect for the thickness of a crust 10%
  Total crust thickness $\Delta R_{\mathrm{crust}}$:
  $M = 1.0M_\odot$ - 2 km
  $M = 1.4M_\odot$ - 1 km
  $M = 1.7M_\odot$ - 500 m

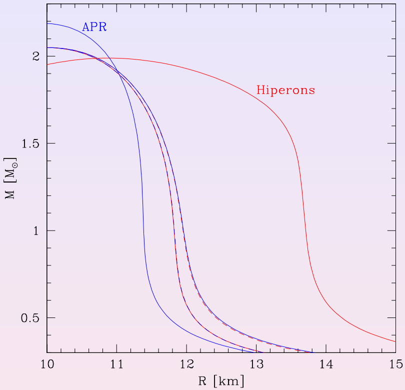

- the difference in radius due to the formation scenario (accreted vs catalyzed crust) much smaller than the effect of the EOS in the core.
- observational inaccuracy of a measurement of a radius of NS larger than 2 km

Observations

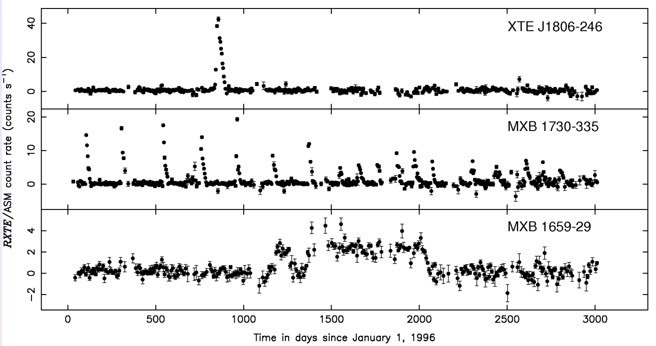

Wijnands 2004

Observations:

- SXT - soft X-ray transients - opportunity to study physics of NS cores and crusts
  - accretion time - days, weeks, quiescence -months, years
  - quiescent emission high - explanation - deep crustal heating
  - explain luminosities of SXT in quiescence
- quasi-persistent SXT- laboratories to study neutron star crusts
  - accretion time - years, decades; then quiescence
  - crust became significantly hotter than in the quiescent phase
  - thermal relaxation between accreting and quiescent stage
  - cooling curve detectable, depends on crust thickness, distribution of heat sources, thermal conductivity

Quasi-persistent soft X-ray transients - example of fits

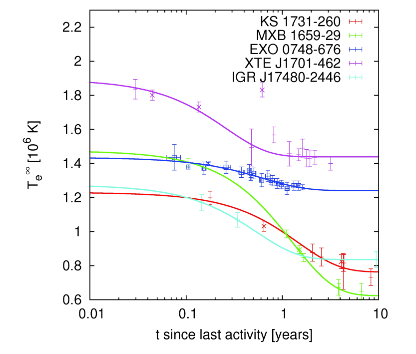

Cooling of quasi-persistent SXT and and fits

Figure from the PhD Thesis of **Morgane Fortin (CAMK, May 2012)**

Problems - shallow sources

New model taking into account H-burning and possibility of **residual accretion**

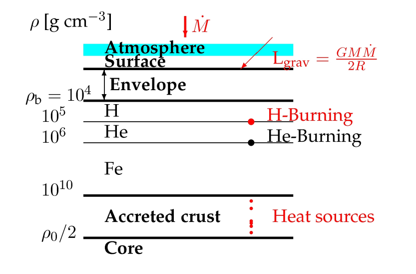

see also A. Turlione, D.N. Aguilera and J. A. Pons, 2013

Q_{tot} and NS cooling

- fitting to KS 1731-260
- 1σ errorbars
- multiplying energy release by 0.5, 2
- the same location of the energy sources

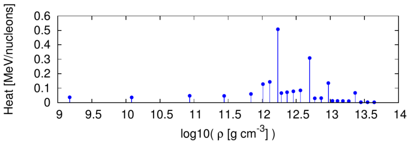

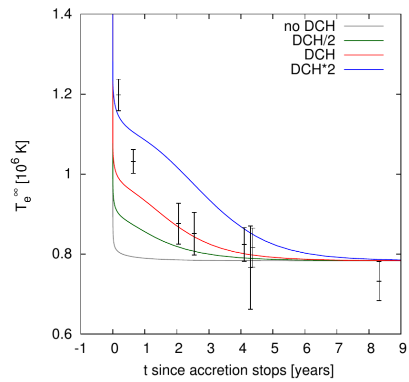

Figures - Morgane Fortin 2014

The role of heat sources location and energy release

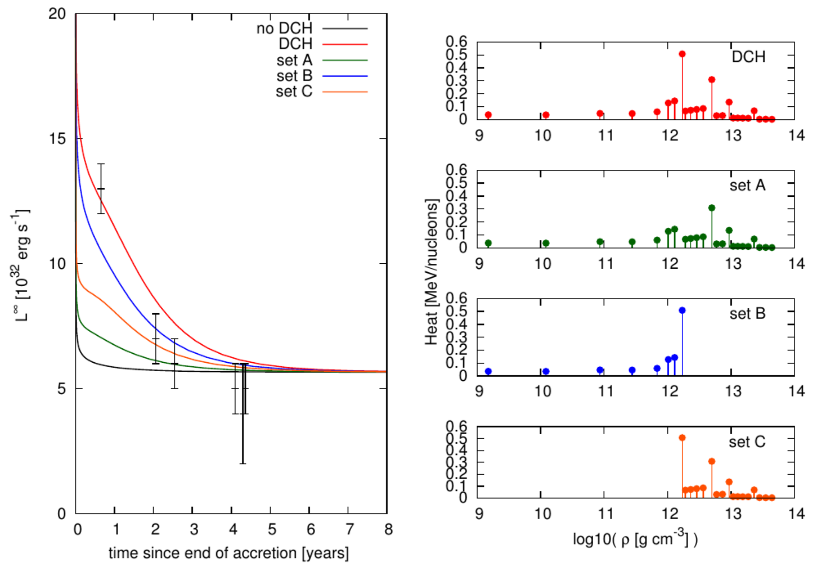

Figures - Morgane Fortin 2014

Problems

Some properties of cooling process cannot be explained by deep crustal heating

- explanation of spectra
  - spectra contaminated by the power law component
  - some sources dominated by non-thermal component
  - non-thermal influence $\rightarrow$ measurement of the luminosity and temperature of the thermal component very complicated
- diversity of QP SXTs - no unique model to explain them - short timescale of cooling for some sources:
  - very different timescales of cooling - from $537 \pm 125\ d$ (KS1731-260) down to $95 \pm 16\ d$ (XTE J1701-462)
  - shallow sources - sources at density $\rho < 10^{10}$ g cm^{-3}
  - residual accretion

Summary

Robust result

Total energy release per accreted nucleon $Q_{\mathrm{tot}} \approx 1.2 - 2$ MeV/nucleon

- total heat release (per one accreted nucleon) weakly depends on uncertainties of the details of deep crustal heating
- total crustal heating is similar for different composition of the ashes of nuclear burning at the surface of accreting NS
- one-component plasma assumption is not crucial
- a chain of processes occurring after the neutron drip leads to convergence of compositions to a common one at densities higher than $5 \cdot 10^{12}$ g cm^{-3} and pressures $P > 10^{31}$erg cm^{-3}.
- main energy sources located at the depth $300 \div 500$ m below NS surface.
- properties of the binding energy of nuclei are important (shell efects vs. even-odd pairing) -
  location of the deep crustal heating, number of energy sources
- importance of the shell effects and even-odd pairing -
  neglecting them lowers Q_{tot} by a factor 2, 3.